

FORCED AND TRAVELING WAVES IN THE MARTIAN ATMOSPHERE FROM MGS TES NADIR DATA.

D. Banfield, *Cornell University, Ithaca, NY USA* (banfield@astro.cornell.edu), **B. Conrath**, *Cornell University*, **R. J. Wilson**, *GFDL*, **M. Smith**, *NASA Goddard*.

Introduction

We have analyzed the temperature retrievals from Mars Global Surveyor (MGS) Thermal Emission Spectrometer (TES) nadir spectra to yield latitude-height resolved maps of various atmospheric forced wave modes as a function of season for nearly two full Mars years. Among the isolated wave modes is the zonal mean, time mean temperature, which we used to derive zonal mean zonal winds and stationary wave quasi-geostrophic indices of refraction, diagnostic of their propagation. The diurnal Kelvin wave was isolated in the data, with results roughly consistent with models (Wilson and Hamilton, 1996). The $s = 1$ and $s = 2$ stationary waves were found to have significant amplitude in ducts extending up the winter polar jets, while the $s = 3$ stationary wave was found to be confined to near the surface. The $s = 1$ stationary wave was found to have little phase tilt with height during northern winter, but significant westward phase tilt with height in the southern winter. This means the wave carries heat poleward in the south, slightly more than that found in Barnes *et al.* (1996). The $s = 1$ stationary wave is the dominant mechanism for eddy meridional heat transport for the southern winter. The forced waves were found to be nearly identical between the first and second years, with the notable exception at time of the large dust storm during the second year ($L_s \sim 185^\circ - 255^\circ$). Much of this appears in Banfield *et al.* (2002).

We have also extracted nearly two full Mars years of traveling wave results. The $m = 1$ wave is the strongest, reaching as high as about 20K in the northern winter polar vortex near solstice. It is much weaker in the south, with peak amplitudes there of about 2K. The $m = 1$ waves are typically centered high in the polar front, but occasionally for very long period (northern) waves, they are coherent all the way to 20S (Wilson *et al.* 2002). $m = 1$ wave periods range from about 2.25 sols to 30 sols. The phase structure of the wave-1 waves shows that they carry a significant amount of heat poleward in the northern winter (especially year 2), and negligible amounts poleward during southern winter. $m = 2$ and $m = 3$ are notably smaller in amplitude than wave-1 throughout the TES nadir data set, rarely exceeding 3K. They are also much more generally confined near the surface, especially $m = 3$, and slightly biased toward the north as well, but much less so than for $m = 1$. Both $m = 2$ and $m = 3$ are slightly stronger in spring than the equivalent time in fall, especially so for $m = 3$. This work will appear in Banfield *et al.* (2003).

Stationary Waves

Figure 1 shows the meridional structure from selected times of the first and second MGS mapping years for stationary waves $m = 1$ and $m = 2$. Here we'll discuss several of the interesting aspects of these waves evident from these plots. Each panel of these plots shows the amplitude and phase of a specific stationary wave, with latitude on the abscissa, and pressure (evenly spaced in scale heights) on the ordinate. Amplitude is indicated by contours, with contours at 1K, 2K, 4K and 8K. Contour color (black or white) is meaningless, changing only to enhance contrast against the background color. The brightness of the background color also indicates amplitude, with bright regions having higher amplitudes. Phase of the stationary wave, given by the longitude of the maximum, is indicated by the hue of the background. Scale bars for the phase are given at the top and bottom (different for $m = 1$ and $m = 2$). The L_s range that the panel represents is indicated on the lower left of each panel. Reading across a row, one sees the meridional structure of either the $m = 1$ or $m = 2$ stationary wave for either the first or second MGS mapping year and 3 different L_s ranges. Comparing the top row to the second allows one to assess interannual variability in the $m = 1$ stationary wave. Similarly for the 3rd row and the bottom row for the $m = 2$ stationary wave. The first column represents a time in early southern spring. The second column represents a time in early northern winter, which also happened to be during a global dust storm that originated in Hellas during the second year. The third column represents a time near the peak of northern winter.

The $m = 1$ wave has its largest amplitudes during the winter seasons in each hemisphere, with a maximum of about 10K in both hemispheres. The maxima are typically found about 3 scale heights above the surface, aligned along the polar front which tilts poleward with height. The polar jet controls the shape of the duct in which the stationary waves can propagate away from the surface. These seasonally exchanging maxima (and the shape of the duct) are evident comparing the first and third columns of the top of Fig. 1. The most significant difference between the north and south maxima is that the phase of the northern wave is nearly constant with height and latitude, very roughly near 220E. In contrast, the phase of the southern wave has a sharp westward tilt with height, shifting some 180 degrees west over a range of 4 scale heights. This indicates a poleward heat transport in the south and essentially none in the north

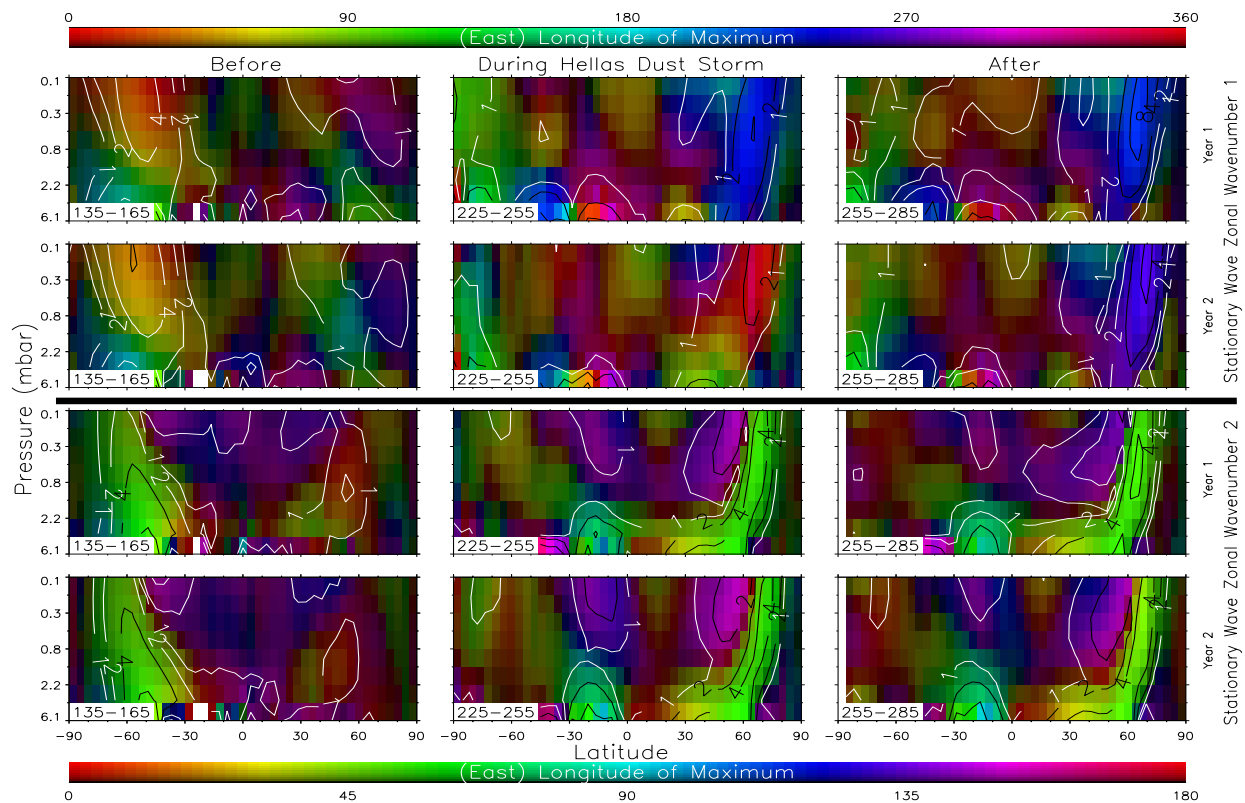


Figure 1: Stationary waves $m = 1$ and $m = 2$ for 3 times over 2 years. Each panel is a meridional cross section and times are arranged down columns. $m = 1$ years 1 and 2 appear in rows 1 and 2 respectively, while $m = 2$ years 1 and 2 appear in rows 3 and 4 respectively. Brightness and contours indicate wave amplitude, while hue indicates longitude of maximum. Colorbars are at the top ($m = 1$) and bottom ($m = 2$). See text for detailed description.

due to the $m = 1$ stationary wave. The $m = 1$ wave likely is the dominant contributor to eddy heat flux in the south, but makes essentially no contribution in the north. There is also a systematic phase tilt eastward with latitude in the south, but not in the north, which represents a momentum transport by the wave that also differs between the hemispheres.

Turning to the $m = 2$ stationary wave, the seasonally exchanging maxima can again be seen comparing the first and third columns of the bottom two rows of Fig. 1. The maxima for $m = 2$ are only slightly smaller than those for $m = 1$, approaching 9K in the north and 6K in the south. The duct for $m = 2$ does not extend to as high altitudes as that for $m = 1$, so the maxima for $m = 2$ are found closer to the surface, below 3 scale heights altitude. The phase of the $m = 2$ stationary wave is nearly a constant at all times of year, and in both the north and south, located at about 60E. This constant phase means that the $m = 2$ stationary wave carries no heat or momentum poleward in either hemisphere, and is inconsequential in the global heat balance within these altitudes. There is, however, an interesting phase shift of 90° just above the edge of the $m = 2$ duct where the

amplitude appears to fall off (in these nadir retrievals). This phase shift is partly responsible for the low observed amplitude (given the tall weighting functions of the nadir retrievals) above the duct, and the consistent behavior in this region suggests that interesting (and somewhat unexpected) phenomena may be happening above our region of sensitivity.

Interannual differences between the first and second years are quite minimal for both stationary waves (comparing the first row to the second, and the third row to the fourth). The behavior is nearly identical in early southern spring (first column) and the peak of northern winter (third column). However, during early northern winter (second column), the global dust storm of the second year appears to have significantly changed the structure of the $m = 1$ stationary wave. Rather than having a constant phase near 220E as it did throughout northern winter in the first year, it has a phase near about 0E, with a marked westward tilt with height. This is a significant change in behavior and clearly points to the global dust storm having strong influences on the $m = 1$ stationary wave (and its ability to carry heat and momentum poleward). Interestingly, the $m = 2$ stationary wave is

essentially unchanged by the presence of the global dust storm. Why it should influence one wave and not the other is unclear.

Traveling Waves

Figure 2 shows the meridional structure from selected times of the first and second MGS mapping years for traveling waves with zonal wavenumbers 1 and 2. Similar to Fig. 1, each panel of these plots shows the amplitude of a specific zonal wavenumber traveling wave, as a function of latitude and pressure. However, also indicated on these panels is the locally dominant period of that traveling wave. Amplitude is again indicated by brightness and contours, with contours at 1K, 2K, 4K every 4K above that. The dominant period of the particular zonal wavenumber wave is shown by the hue of the background. Scale bars for the period are given at the top and bottom (different for $m = 1$ and $m = 2$) and negative periods in the scale bar (only) indicate westward propagation. Otherwise, the overall structure of Fig. 2 is very similar to Fig. 1. Again, the first column represents a time in early southern spring. This time, the second column represents a time in northern fall, just after the onset of the global dust storm during the second year. The third column again represents a time near the peak of northern winter.

The most striking aspect of the $m = 1$ traveling wave is the hemispheric dichotomy in the peak amplitudes. The north has its peak amplitude near the peak of winter, aligned along the polar front with a maximum at about 3 scale heights altitude, much like the $m = 1$ stationary wave. The northern peak amplitudes are about 12K the first year and about 20K the second year. The south however only reaches about 2K for the $m = 1$ traveling wave in any of the MGS data analyzed. The amplitude is generally strongest near southern winter, but not nearly as dramatically so as in the north. The southern waves have periods from as fast as about 3 sols, to as slow as about 25 sols, sometimes westward. Occasionally, waves in both hemispheres appear to have two distinct periods, one faster wave near the surface and a slower one at altitude.

The large northern winter $m = 1$ waves have periods that are as slow as about 30 sols. Secular trends of lengthening periods have been identified in these waves, especially in the second year, which can be described as “chirping,” as it goes from a period near 8 sols all the way down to about 30 sols, while still remaining a coherent and identifiable wave throughout this time. The meridional extent of these slow waves is also not limited to the vicinity of the polar front. The waves are coherent, and have measurable amplitude of greater than 1K extending across the equator to as far as 20S, in both the first and second MGS mapping years (e.g., column 3, row 2 of Fig. 2). In the first year, the slow

(20-30 sol) wave was quickly replaced by a faster (7 sol) $m = 1$ traveling wave which had grown from below (Wilson *et al.* 2002) (note blue region at 50N near the surface in column 3, row 1 of Fig. 2). The slow waves have little amplitude near the surface, and thus have little surface pressure expression, explaining their absence in the Viking Met data. At the same time, in the south, there are westward propagating $m = 1$ traveling waves with a period of about 13 sols. The amplitudes are less than 2K, but the behavior seems to be repeatable from year to year.

Interannual variability in the $m = 1$ traveling wave is significant. While the general trend of strong, slow northern winter waves appears repeatable, the absolute amplitude changed by nearly a factor of 2, and the periods vary by large amounts in different ways between the two years examined. The southern waves also appear to be consistently small, but the specifics of the periods and amplitudes vary considerably from one year to the next. Only the westward traveling waves in the southern summer appear to be repeatable in both amplitude and period between the two years. The global dust storm of the second year (row 2, column 2 in Fig. 2.) causes 2K, 18 sol traveling waves in the midlatitudes of both hemispheres. The perturbations are maximum at the top of our domain at about 60S and 60N, and they move in phase in both hemispheres for about 1 full period (this isn't clear in Fig. 2 due to an averaging time longer than this). How the dust storm causes this globally coherent traveling wave is not clear.

The phase structure of the $m = 1$ traveling waves in the northern winter (not shown) have a marked westward tilt with height, indicating poleward heat transport. Recall that the $m = 1$ stationary wave carried relatively little heat poleward in the northern winter, despite its substantial amplitude. The $m = 1$ traveling wave carries only slightly more heat poleward in the first year than the $m = 1$ stationary wave. But during the second year, especially during early northern winter, the $m = 1$ traveling wave clearly dominates the eddy poleward heat flux, carrying 5-10 times the flux from the higher zonal harmonic traveling waves or the stationary waves. Thus, the $m = 1$ traveling wave is the dominant contributor to eddy heat flux in the north with strong interannual variability. However, its small amplitudes during southern winter confirms that the $m = 1$ stationary wave is the dominant component there. The phase tilt with *latitude* varies depending on the altitude considered, suggesting that momentum is being transported poleward at some altitudes and equatorward at others.

The $m = 2$ traveling waves and the $m = 3$ traveling waves (not shown) are much weaker than the $m = 1$ (northern winter) traveling waves. Their amplitudes are less than 4K throughout our observations, more typically maxima are about 2K. The $m = 2$ waves are somewhat more confined near the surface than the $m = 1$ traveling waves, not surprisingly much like the differ-

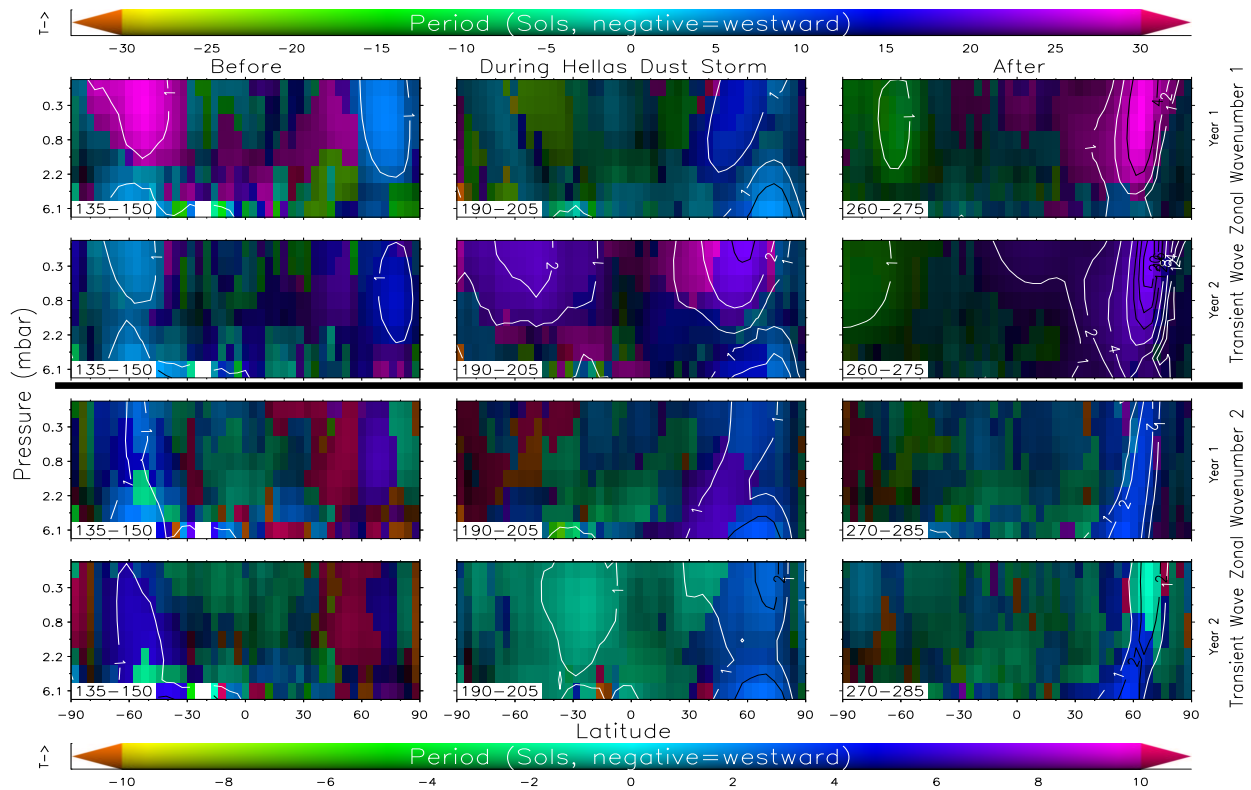


Figure 2: Traveling waves $m = 1$ and $m = 2$ for three different times over two different years. The overall structure of this figure is nearly identical to Fig. 1. Amplitudes are again brightness and contours, while hue indicates the period of the dominant wave. See text for detailed description.

ences between the $m = 1$ and $m = 2$ stationary waves. The similarity continues through to the $m = 3$ traveling waves, being essentially trapped in the bottom scale height of the atmosphere, although the traveling waves appear slightly less vertically trapped than their stationary wave kin. Perhaps the occasional $m = 3$ traveling waves seen at altitude are generated in situ at altitude. Results for $L_s \sim 140^\circ$ of year 1 near 70S are consistent with Hinson and Wilson (2002) where they find a $m = 3$ traveling wave with a period of about 2 sols and an amplitude of about 2K. The $m = 2$ traveling waves are slightly favored in the north over the south, with amplitudes about twice as large in the north. Periods range from about 2.3 sols to about 5.5 sols. During the global dust storm, our results show a westward $m = 2$ traveling wave with a period of just over 1 sol (row 4, column 2 of Fig. 2), but we have not yet determined whether that is real or an artifact. The broad region over which it appears coherently and its coincidence with the dust storm suggest it might be real. We also occasionally find fast westward traveling $m = 2$ waves in the vicinity of the polar front, just where and when the $m = 1$ traveling

wave is having its maximum amplitudes (row 4, column 3 of Fig. 2). In this case as well, we have not yet determined whether this is real or an artifact, due to the considerable dominance of the $m = 1$ traveling wave in this region and time. Heat fluxes due to the $m = 2$ and $m = 3$ traveling waves can generally be ignored relative to the $m = 1$ stationary and traveling waves (for the southern and northern winters respectively).

This work is supported by NASA's MDAP program.

References

- Banfield *et al.*, 2002. *Icarus*, in press.
- Banfield *et al.*, 2003. *Icarus* Submitted.
- Barnes *et al.*, 1996. *J. Geophys. Res.* **101**, 12753-12776.
- Hinson and Wilson, 2002. *GRL* 10.1029/2001GL014103.
- Wilson *et al.*, 2002. *GRL* 10.1029/2002GL014866.
- Wilson and Hamilton, 1996. *J. Atmos. Sci.* **53**, 1290-1326.